

Effect of CO₂ phase on CO₂ storage at pore level”

Professor Xianfeng Fan

E-mail: x.fan@ed.ac.uk

School of Engineering

The University of Edinburgh

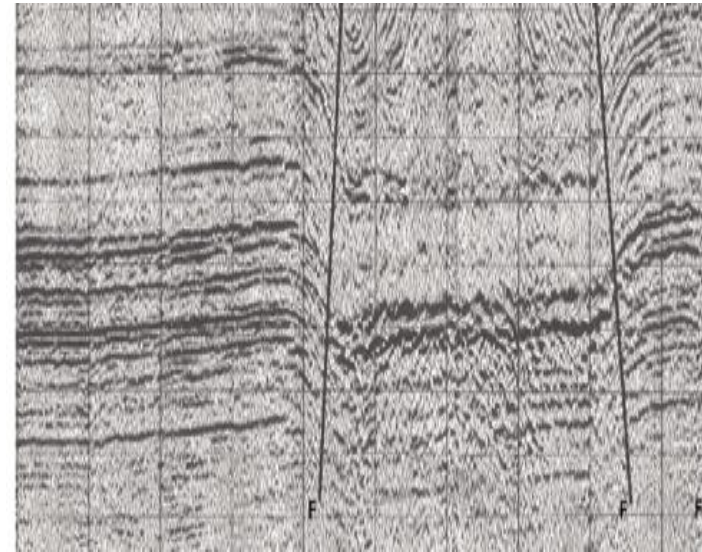
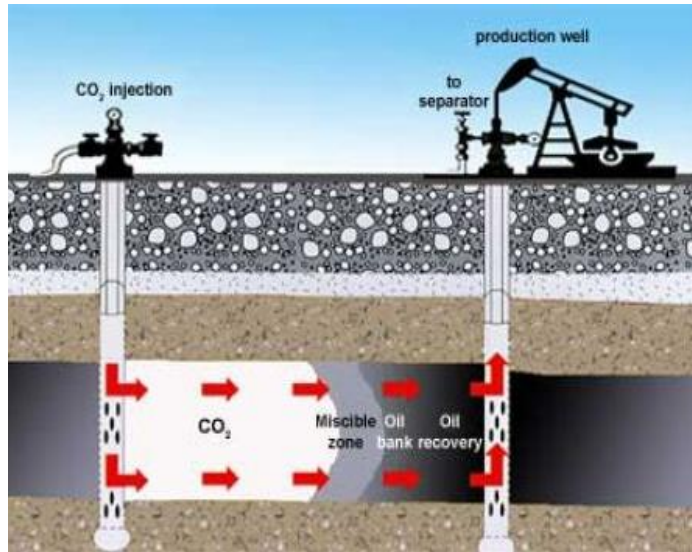
Research Activities and Interests

Research activities in my group

- Multiphase phase flow in porous media for CO₂ storage and enhanced oil recovery
- CO₂ capture
- Fluidization and mixing,
- Photocatalysis for waste water treatment and CO₂ reforming

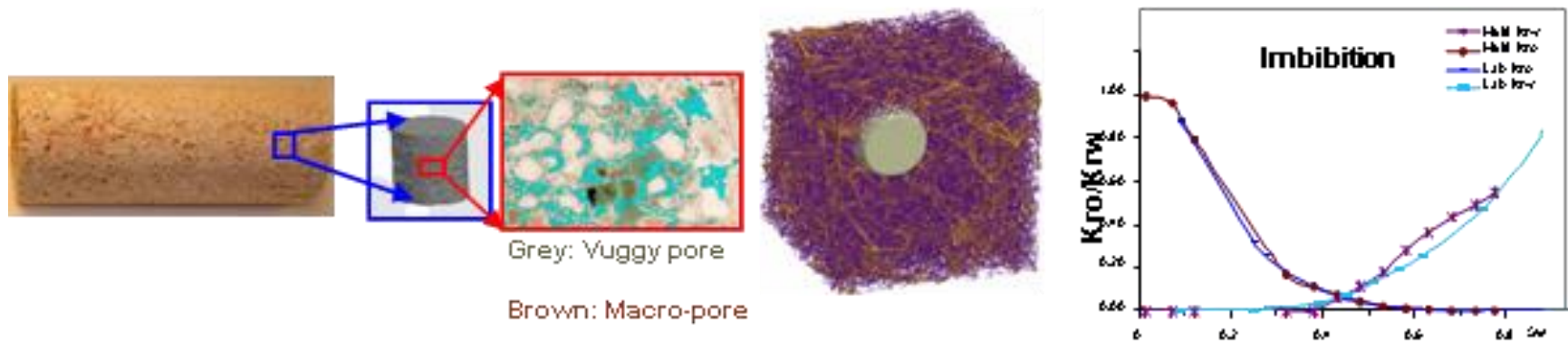
Work forming today's talk is from Miss Cong Chao, Dr Xingxun Li, Dr Claudia Martin

Oil/CO₂ displacement and migration at geological fault and pores, and pores,



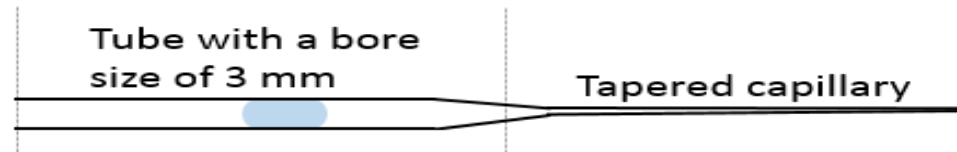
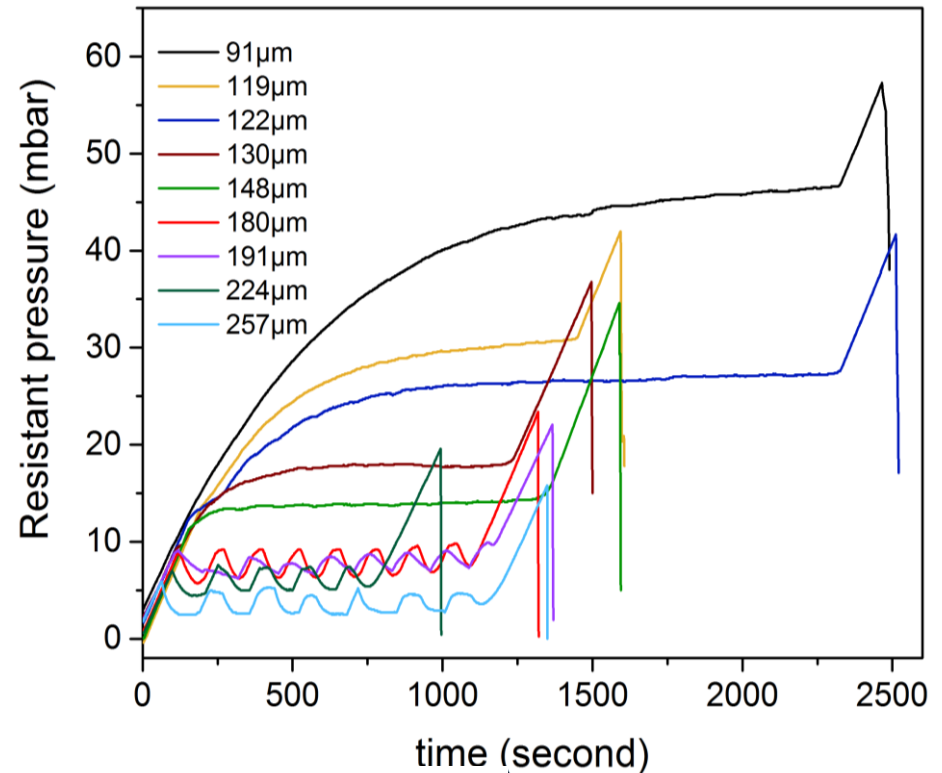
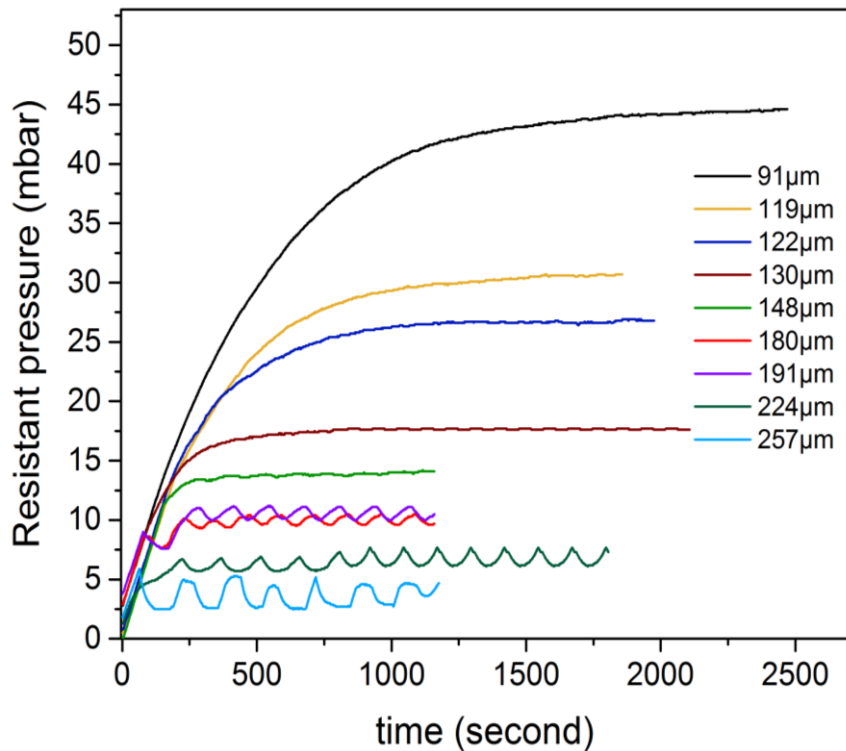
- CO₂ storage is a displacement process at pore and geological faults
- It is a geologic scale engineering, but controlled at pore level.

Study oil/CO₂ displacement and migration at geological fault and pores,

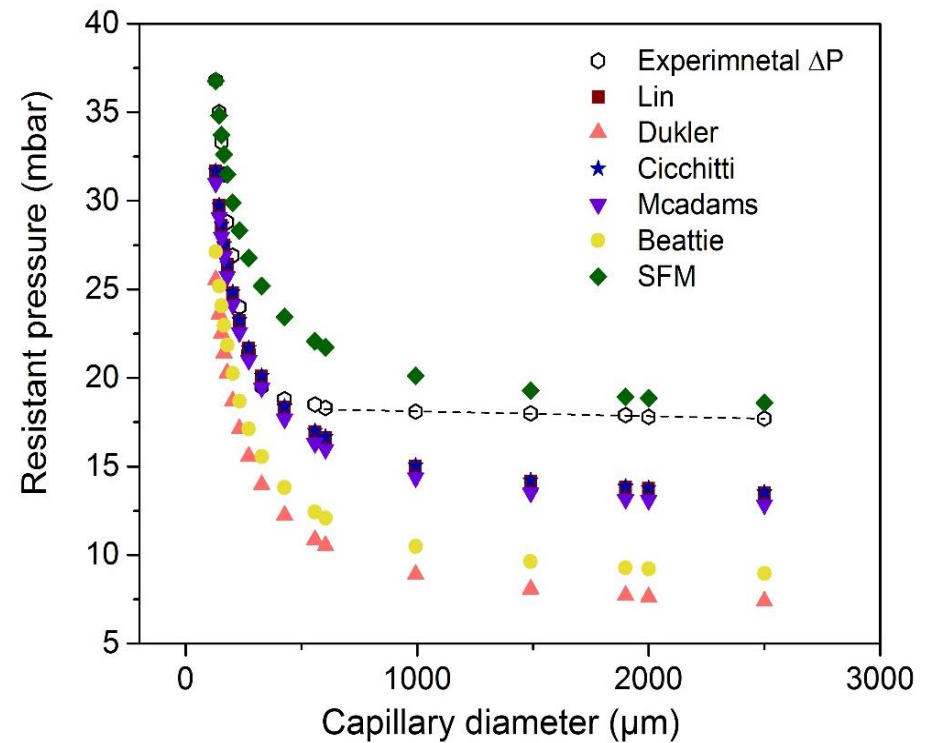
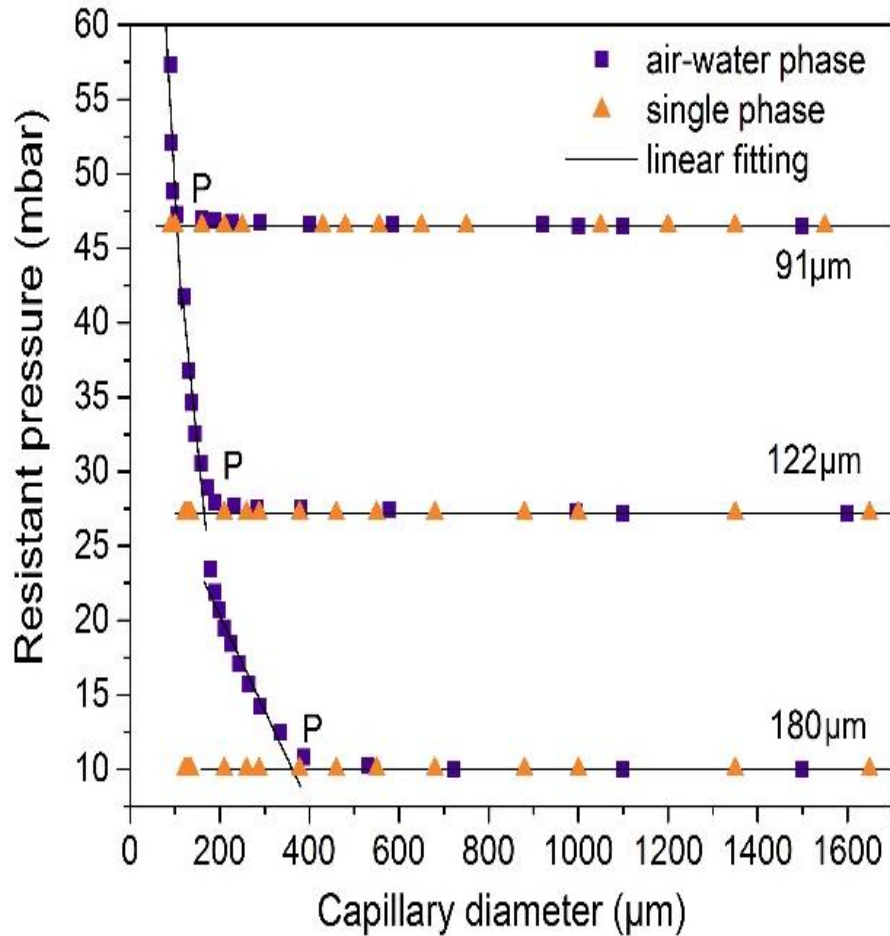


- Displacement is controlled by pore structure, pore wettability, pore surface chemistry, interaction between pore surface, water, oil, CO₂
- Core scale study gives statistic data of the displacement and migration.
- Permeability is a summery of the effect of many factors

Pressure resistance to single and two phase flows in a capillary (Miss Cong Chao)



Pressure resistance to single and two phase flows in a capillary



Prediction of the pressure resistance from the tapered capillary



$$\Delta P = \Delta P_{f1} + \Delta P_{f2} + \Delta P_c + \Delta P_{contraction} - \frac{\rho}{2} (u_1^2 - u_2^2)$$

where ΔP_{f1} is the frictional pressure drop in the tube with an inner diameter of 3 mm,

ΔP_{f2} is the frictional pressure drop for fluid flowing through the tapered capillary,

$\Delta P_{contraction}$ is the pressure loss due to the sudden contraction

ΔP_c is the capillary pressure.

u_1 and u_2 are the mean fluid superficial velocity in the tube with an inner diameter of 3 mm and at the tip point of a tapered capillary, respectively.

Prediction of the pressure resistance from the tapered capillary

Frictional pressure was predicted based on homogeneous flow model and separated flow model

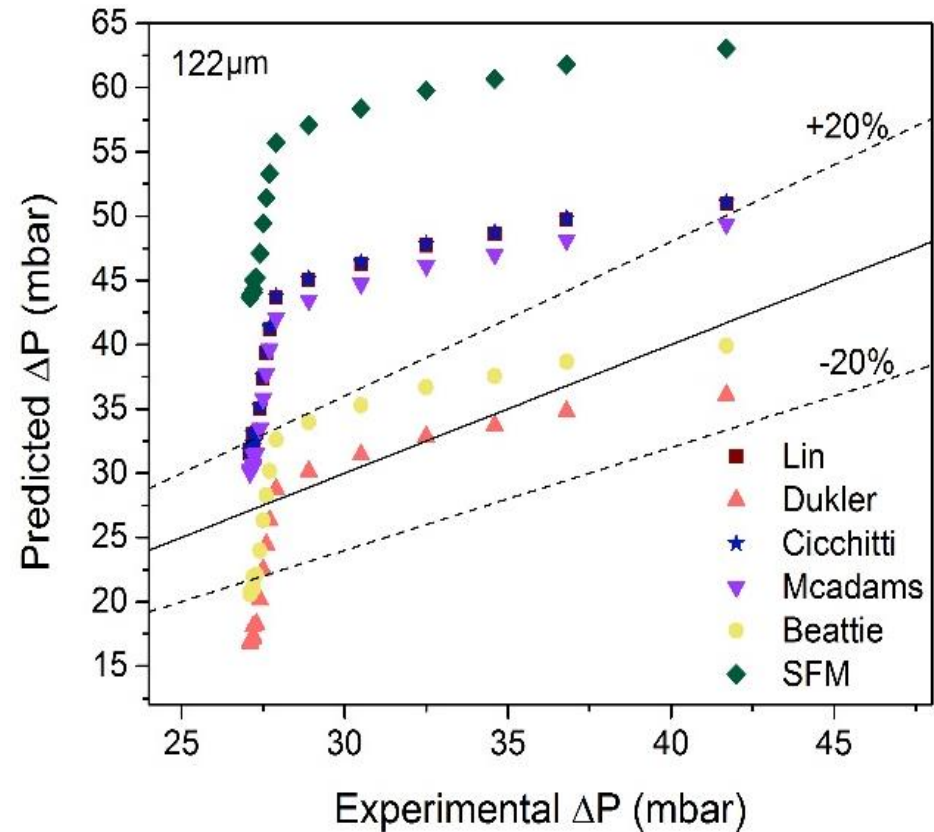
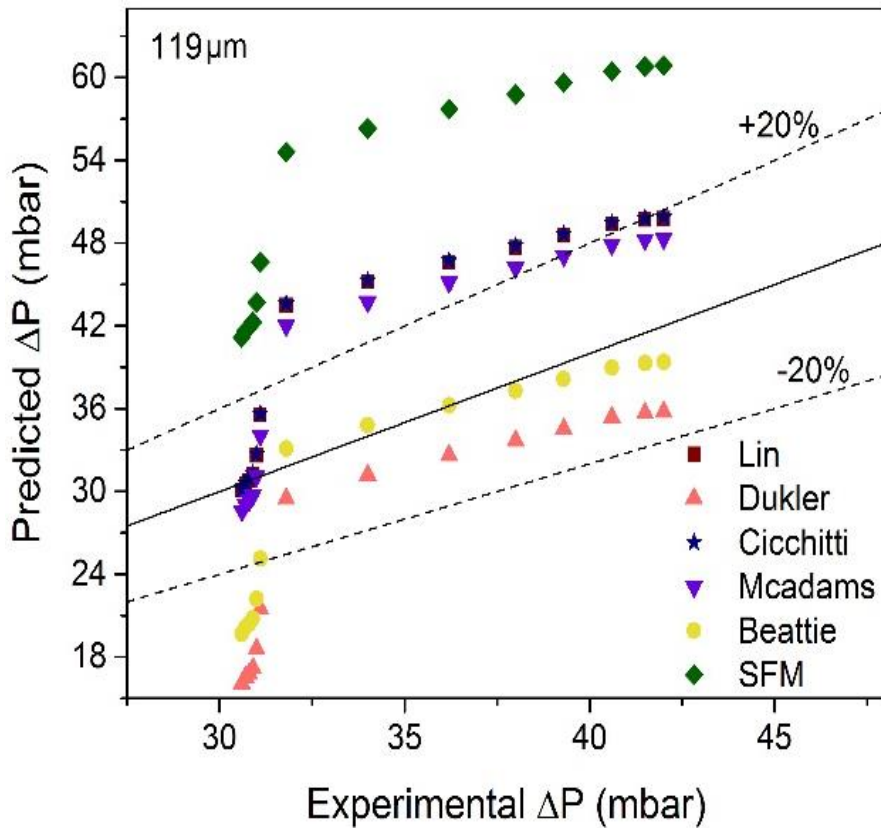
$$\Delta P_{TP} = \frac{f_{TP} \rho_m Q^2}{\pi^2 k r^4} = 32 \frac{\mu_m Q}{\pi k r^3} \quad \Delta P_{TP} = \phi^2 \Delta P_{SP} = \phi^2 \frac{f \rho_l Q^2}{\pi^2 k r^4}$$

Pressure drop due to the sudden contraction

$$\Delta P_{contraction} = \frac{G^2}{2\rho_l} \left[\left(\frac{1}{C_C} - 1 \right)^2 + 1 - K^2 \right] \left[1 + x \left(\frac{\rho_l}{\rho_g} - 1 \right) \right]$$

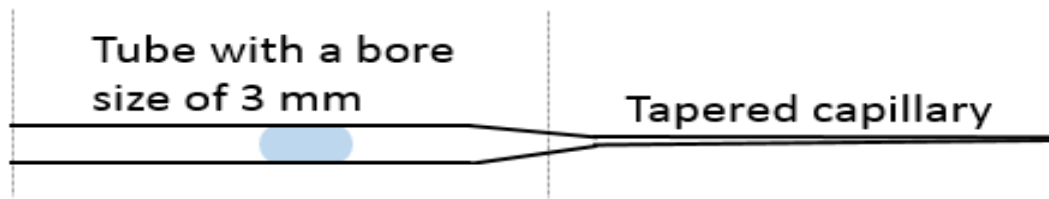
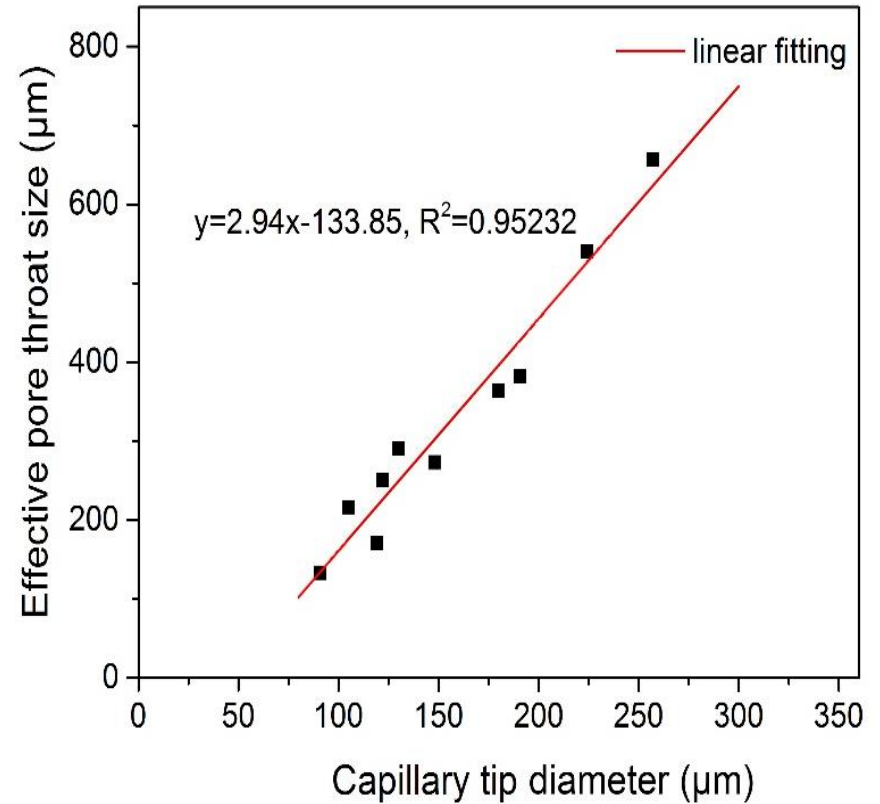
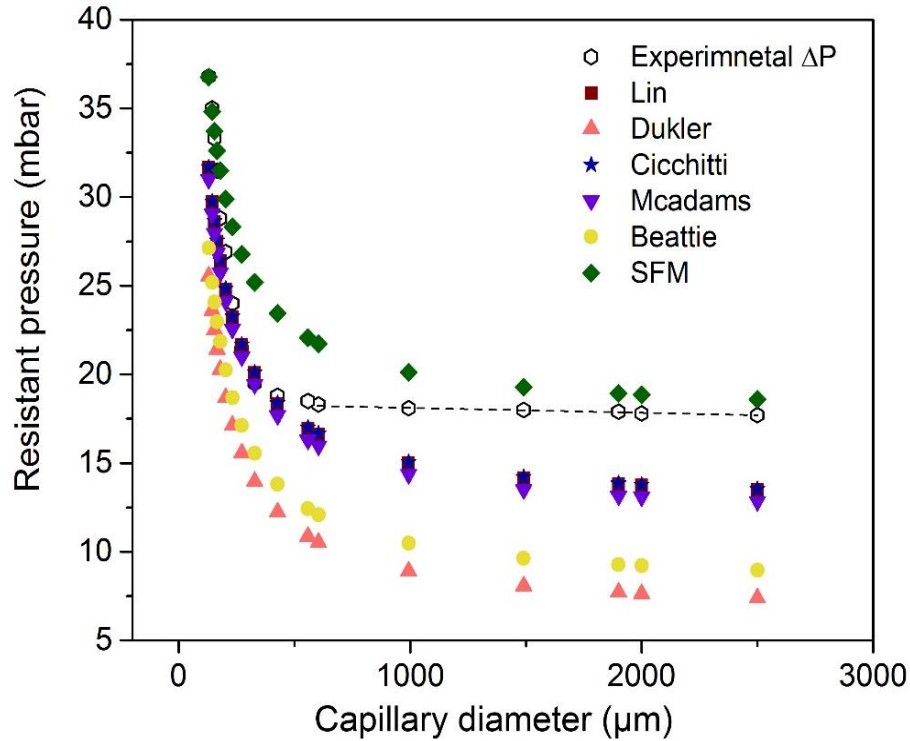
Capillary pressure

$$P_c = \frac{2\gamma \cos\theta}{r}$$



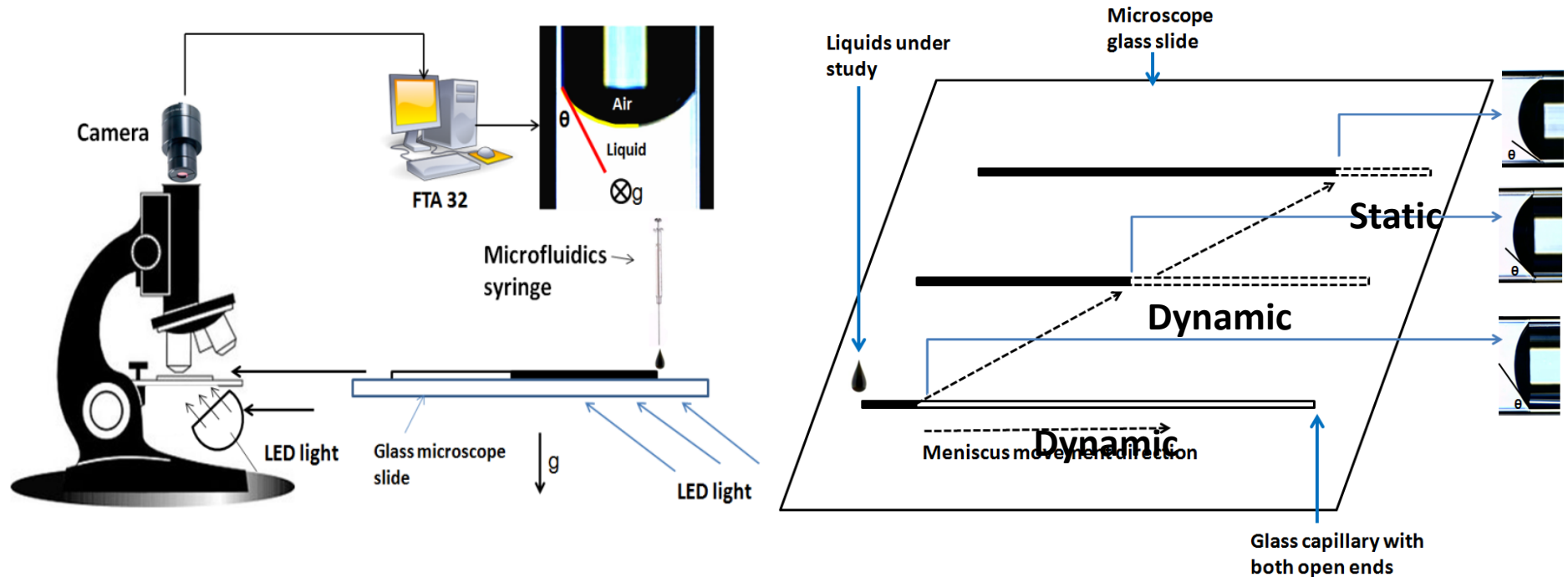
Experimentally measured pressure drop versus the predicted pressure for two-phase flows in tapered capillaries with tip size ranging from 91 to 257 μm

Effective Pore throat



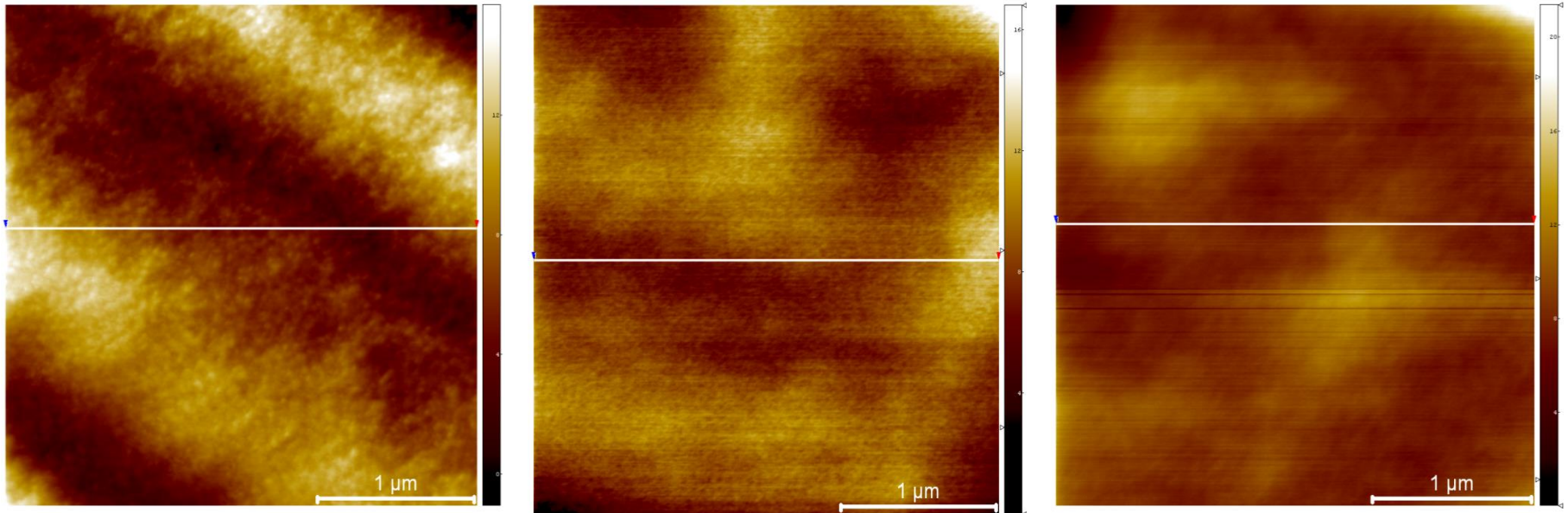
Measurement of pore wetting

Dr xingxun Li



This microscopic image technique developed in our lab works very well for contact angle measurements of liquids in a small pore. This technique has been used for static pore wetting, dynamic pore wetting, chemical structure effect on pore wetting, pore wettability alteration studies and also applied to reservoir liquid-CO₂ pore wetting under high pressure.

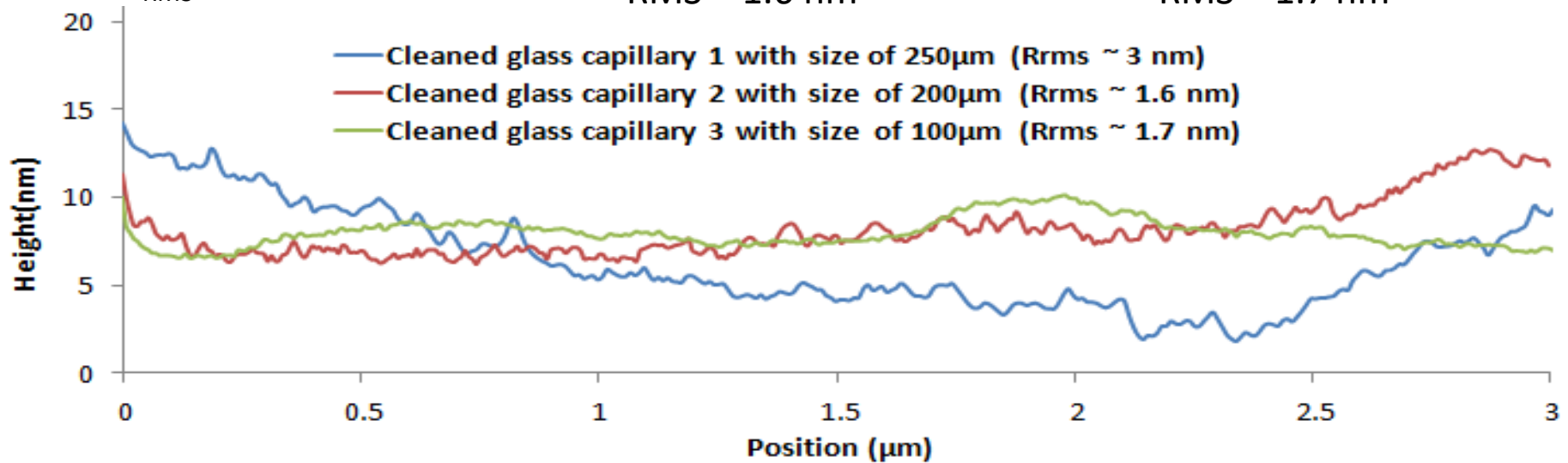
Roughness of Inner Pore Surface by AFM



$R_{\text{RMS}} \sim 3 \text{ nm}$

RMS $\sim 1.6 \text{ nm}$

RMS $\sim 1.7 \text{ nm}$



Pore Wetting -- Static Pore Contact Angle

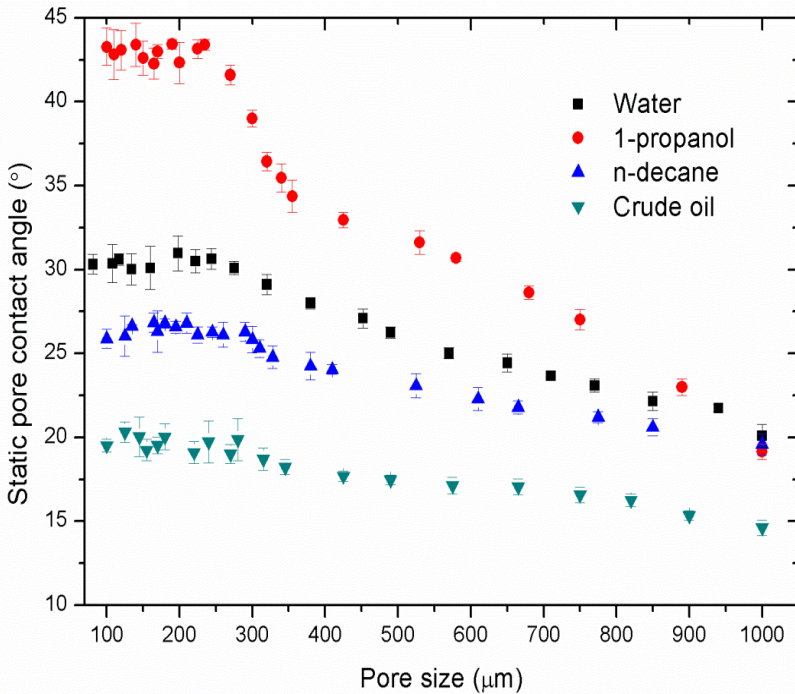
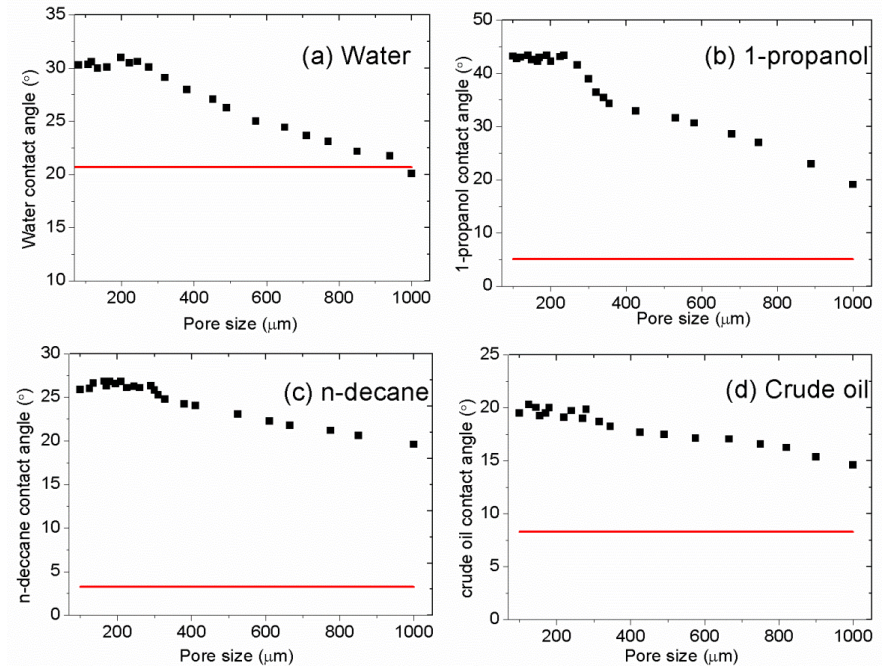


Fig.1 Effect of pore size on static pore wetting

- Pore contact angle varies with pore size.
- Contact angles in pores are largely different from the contact angles measured from flat surfaces.
- Chemical structure of liquid might affect its contact angle in a glass pore



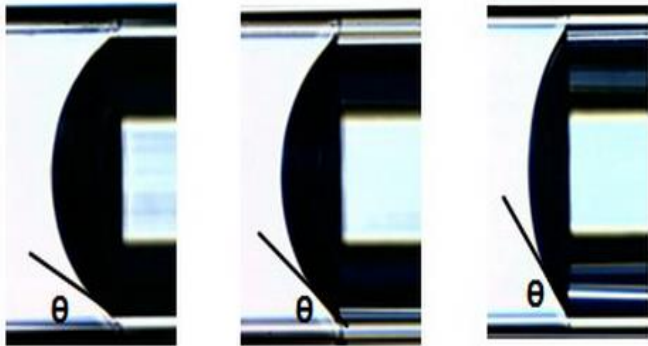
■ Pore contact angle — Contact angle on a flat surface.



Fig.2 The difference between contact angles measured in a pore and on a flat surface

Dynamic pore contact angles

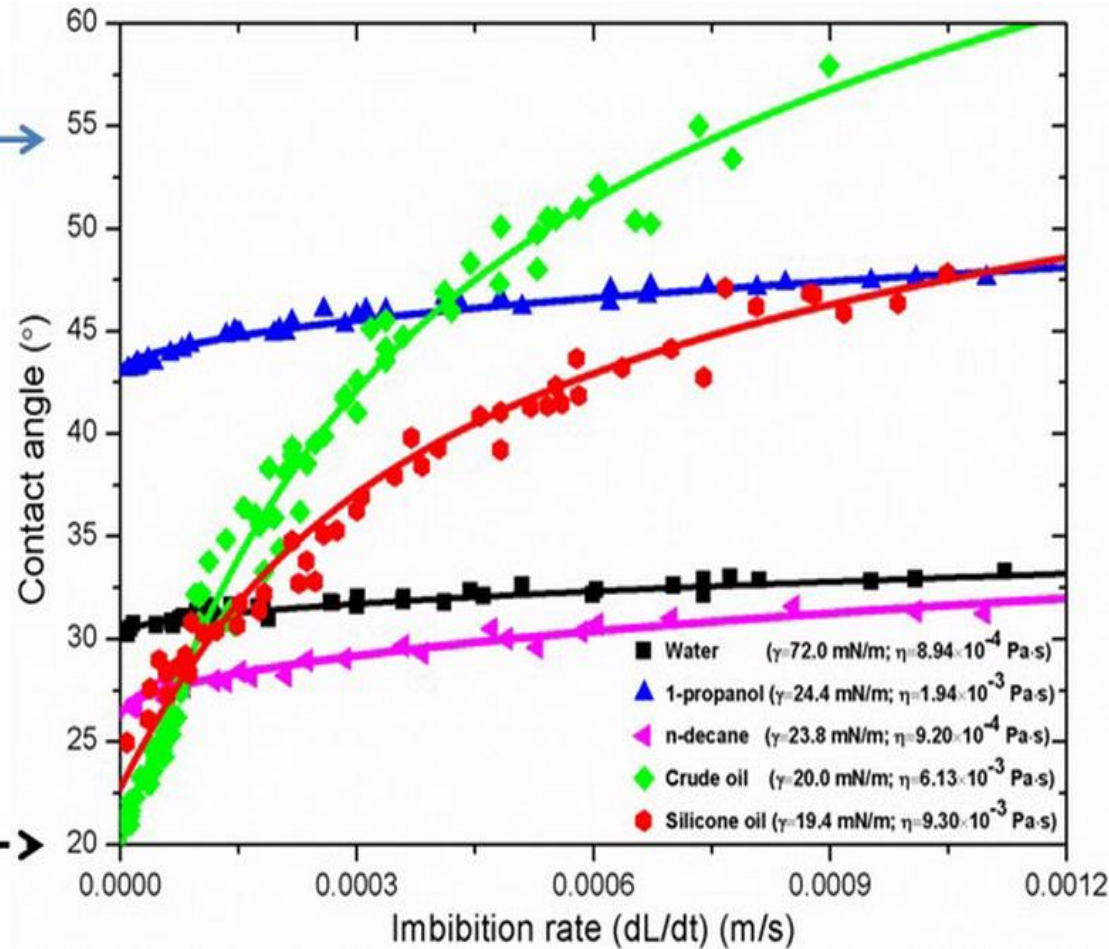
- Surface tension (γ)
 - Viscosity (η)
- effect →



Static

Dynamic

Imbibition rate (dL/dt)



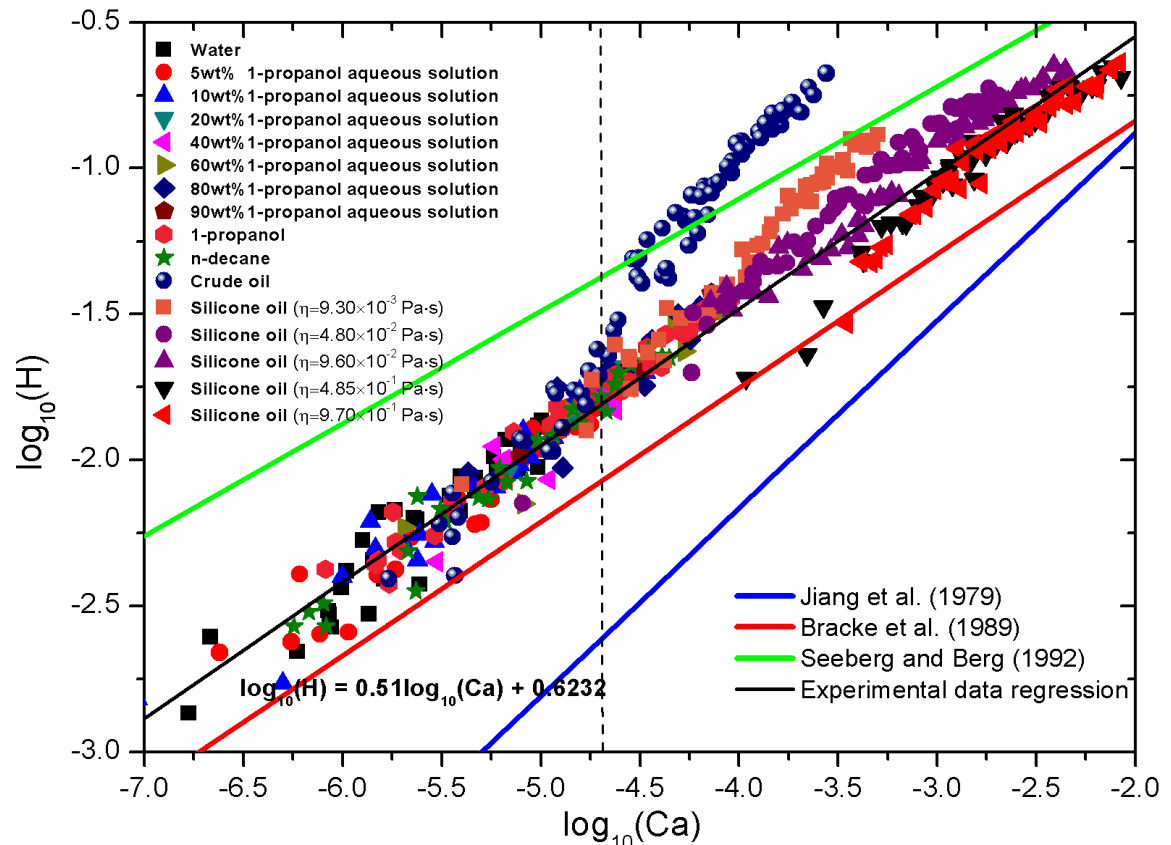
Effects of imbibition rate, surface tension and viscosity on dynamic pore contact angle

Dynamic pore contact angles

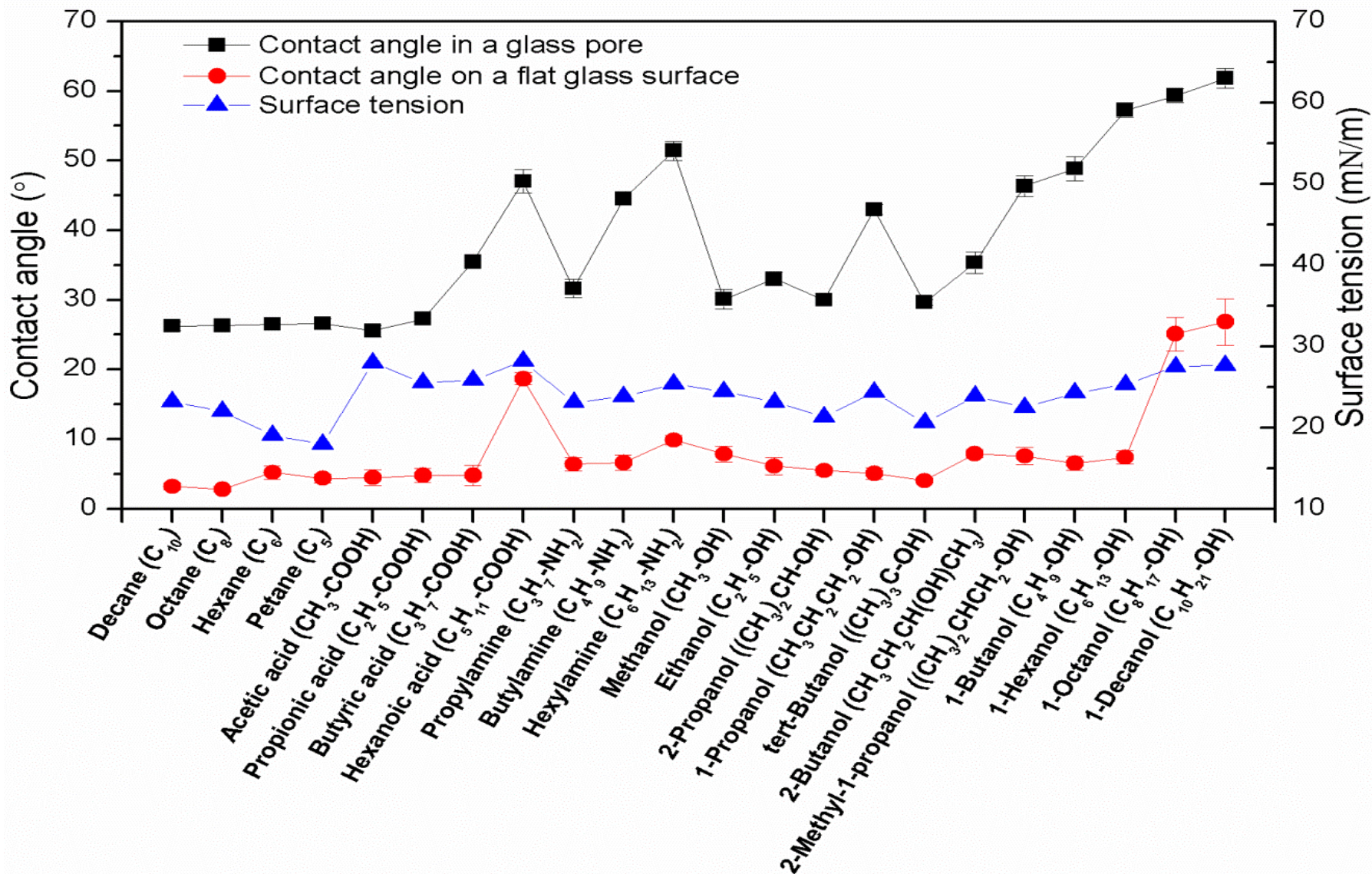
- Dynamic contact angle of liquids in a pore depends on and contact-line velocity, surface tension and viscosity of liquids.
- A new empirical correlation proposed based on our experimental data can predict the dynamic contact angles for liquids in a small pore at a low capillary regime ($1.0 \times 10^{-7} < Ca < 1.8 \times 10^{-5}$).

$$H = 4.2 Ca^{0.51}$$

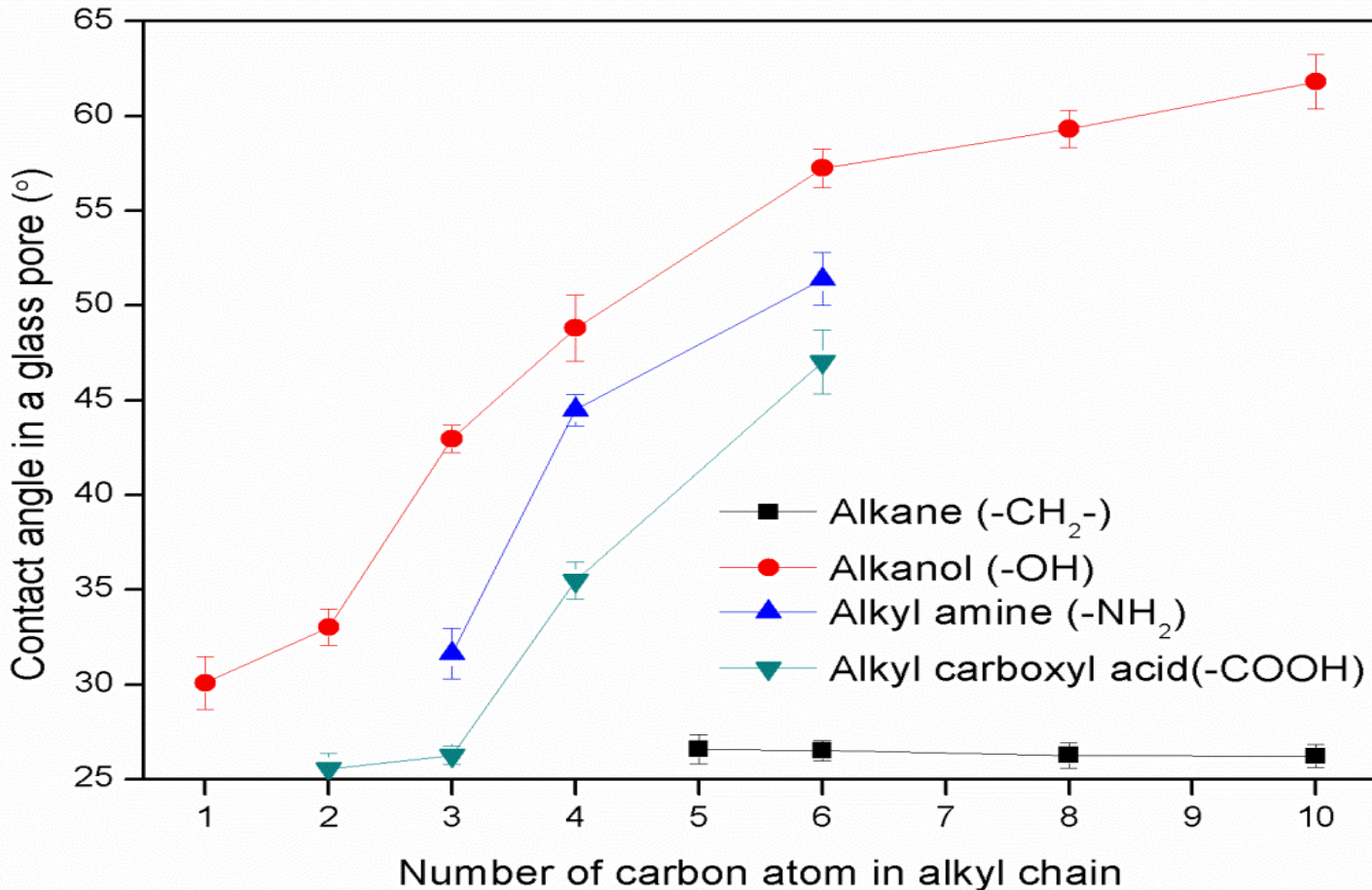
$$H = \frac{\cos\theta_s - \cos\theta_d}{\cos\theta_s + 1} = A Ca^B$$



Effect of Chemical Structure on Pore Wetting

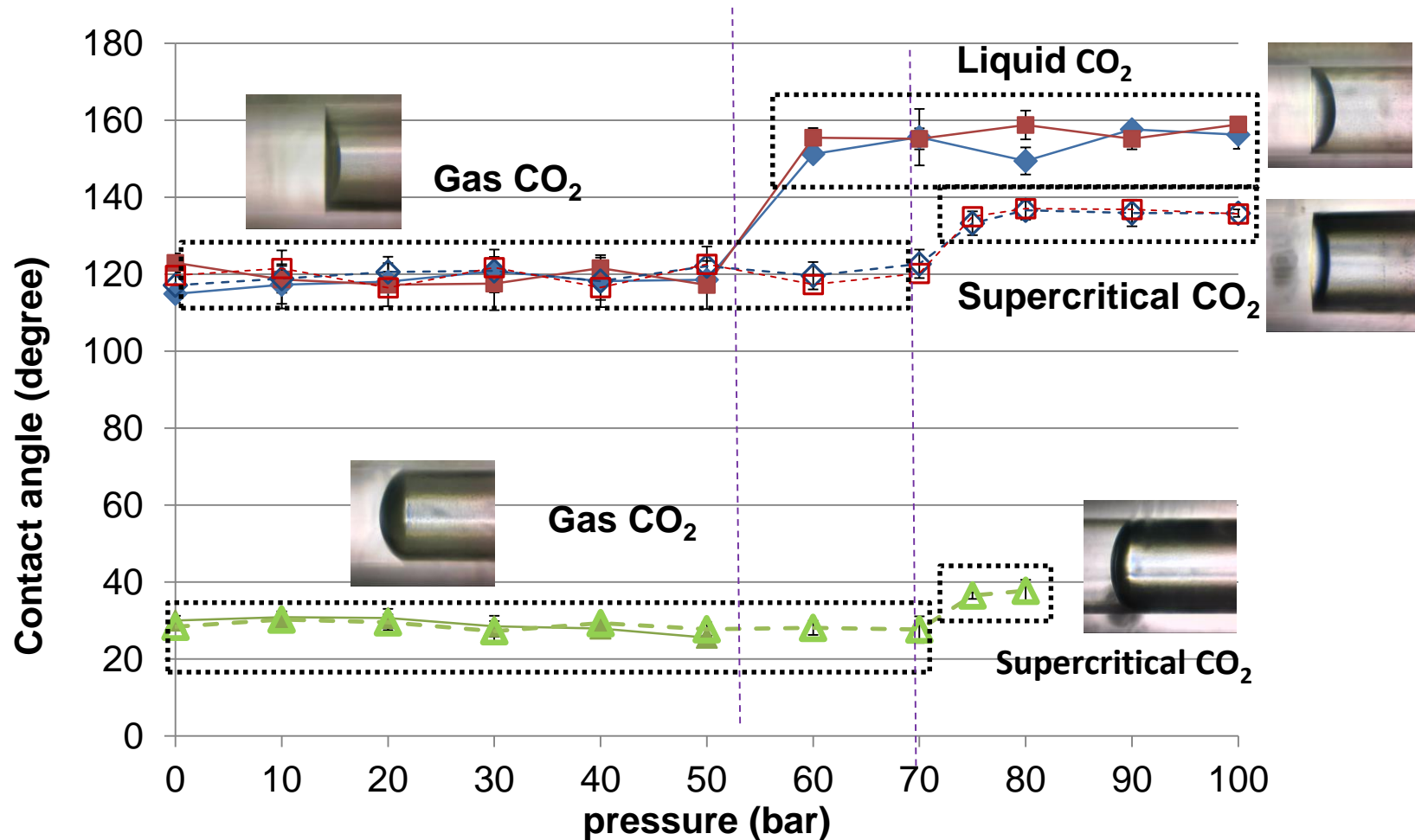


Effect of Alkyl Chain Length on Pore Wetting



The pore contact angle of non-polar organics does not depend on the alkyl chain length. The pore contact angle of amphiphiles increases dramatically with the straight alkyl chain length.

Pore Wetting of CO₂ –water-brine-n-decane



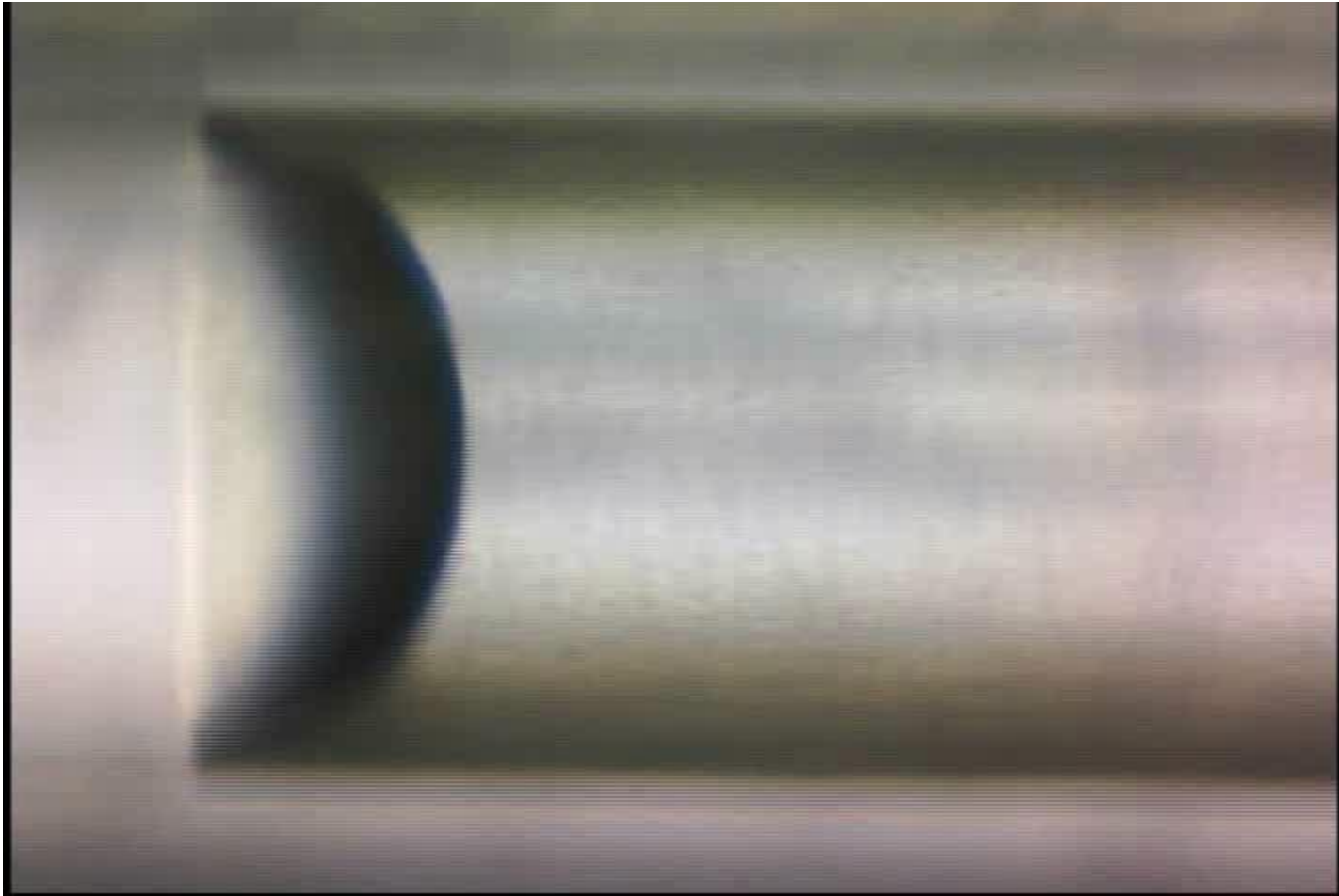
- FEP is a hydrophobic material, which could represent the oil-wet mineral surface in an oil reservoir. The CO₂ turns from gas phase to liquid phase at approximately 60 bars.
- The wetting property of liquid CO₂ is different from gas CO₂ in the FEP pores.
- Salinity effect is not significant on pore wetting in this FEP pore.

Water, Gas and Liquid CO₂ in a Capillary Tube



Increase pressure from 55 bar

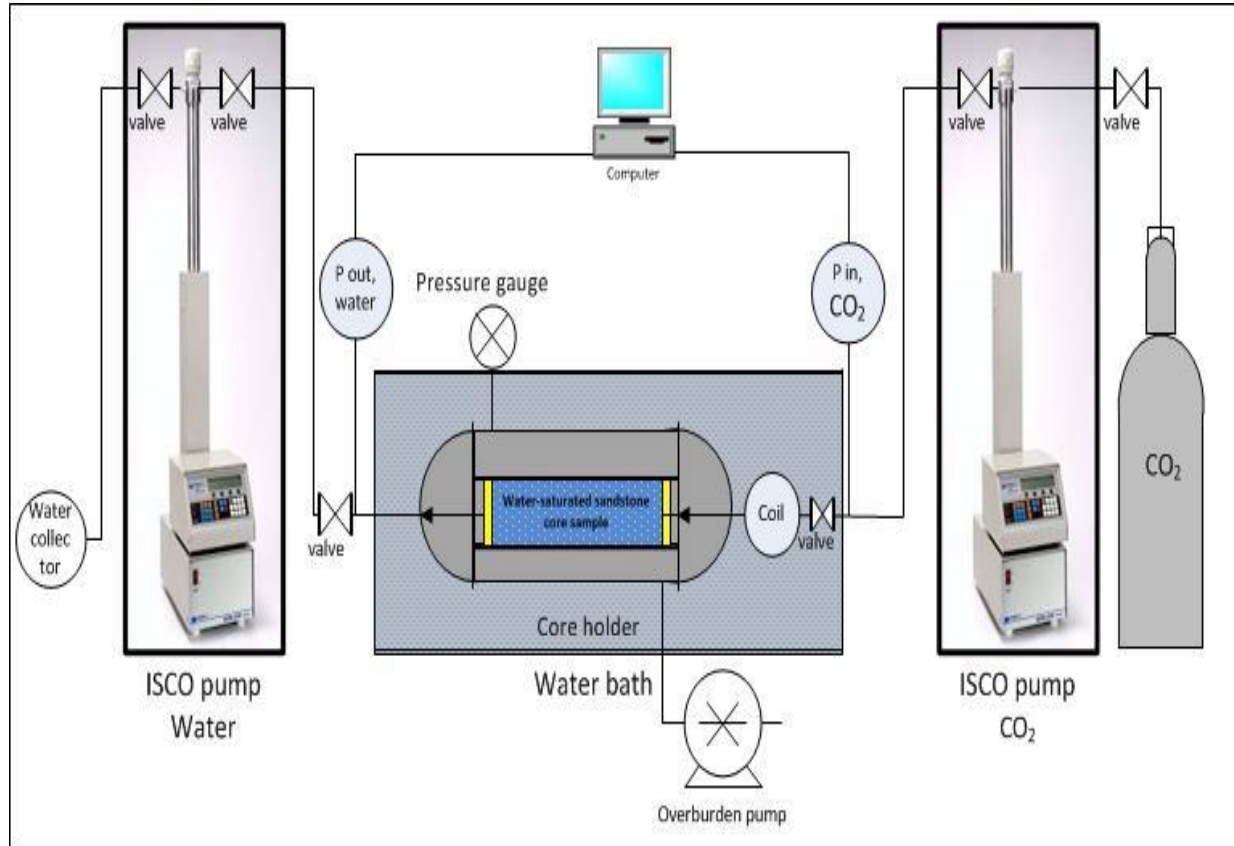
Water, Gas and Liquid CO₂ in a Capillary Tube



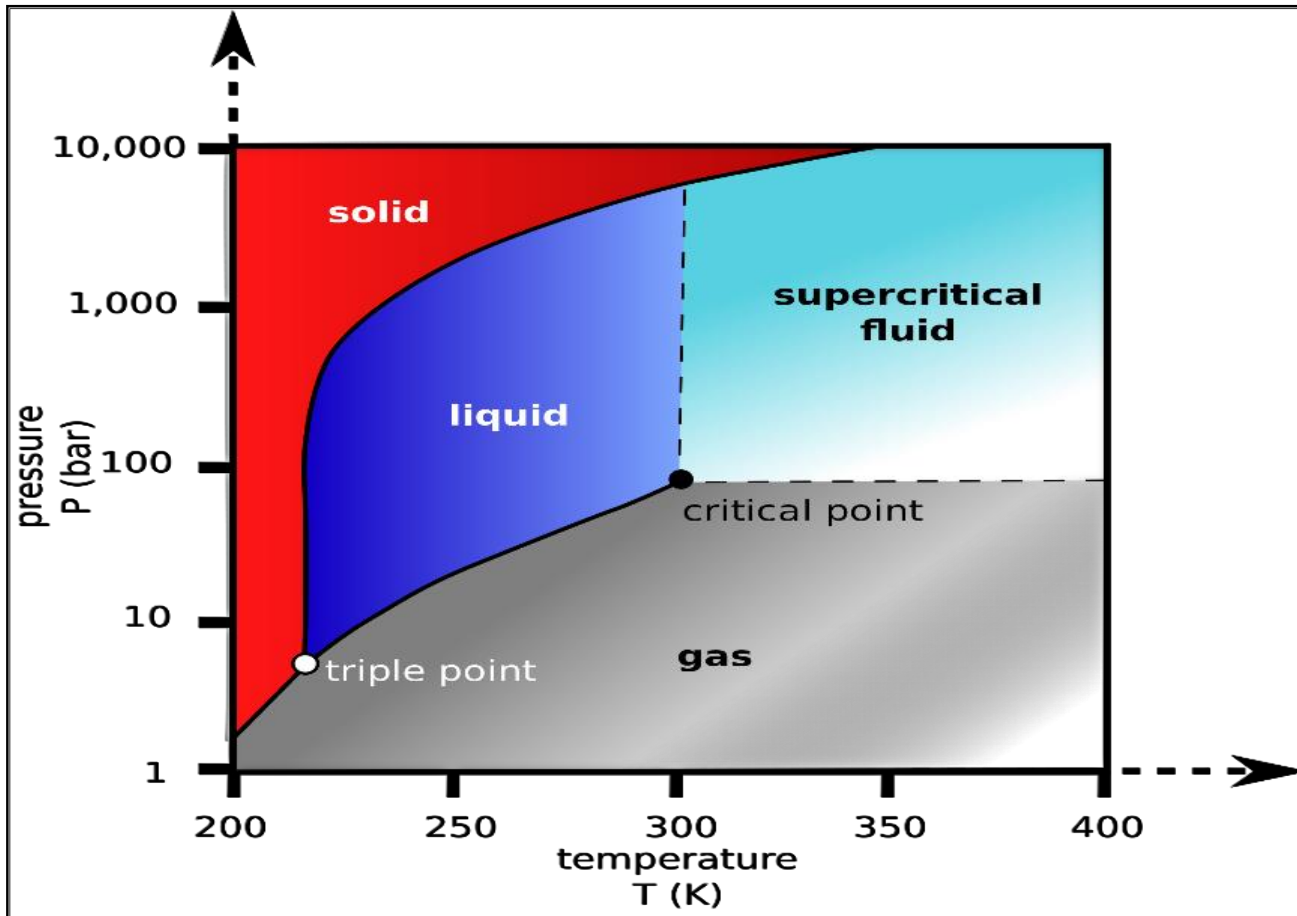
Decrease pressure from 60 bar

Effect of CO₂ phase on CO₂-water displacement

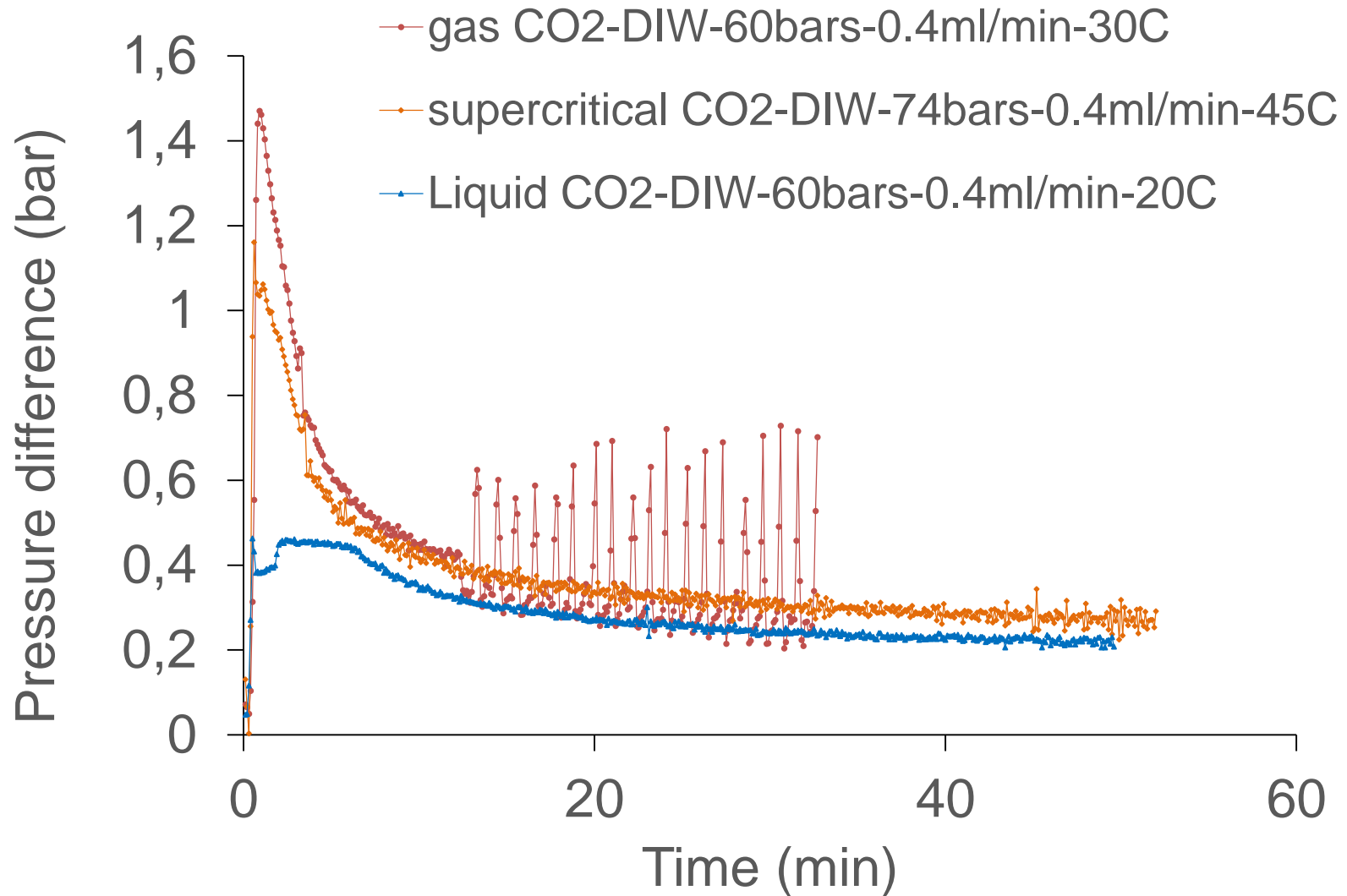
Dr Xingxun Li, Mr Al-Zaidi



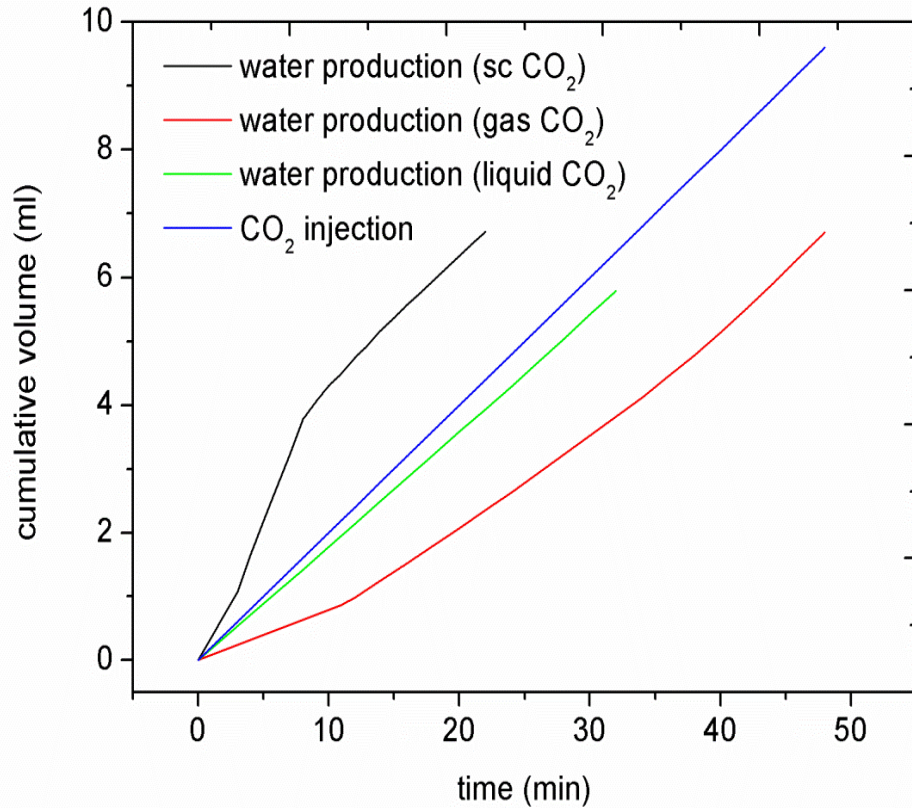
CO₂ Phase



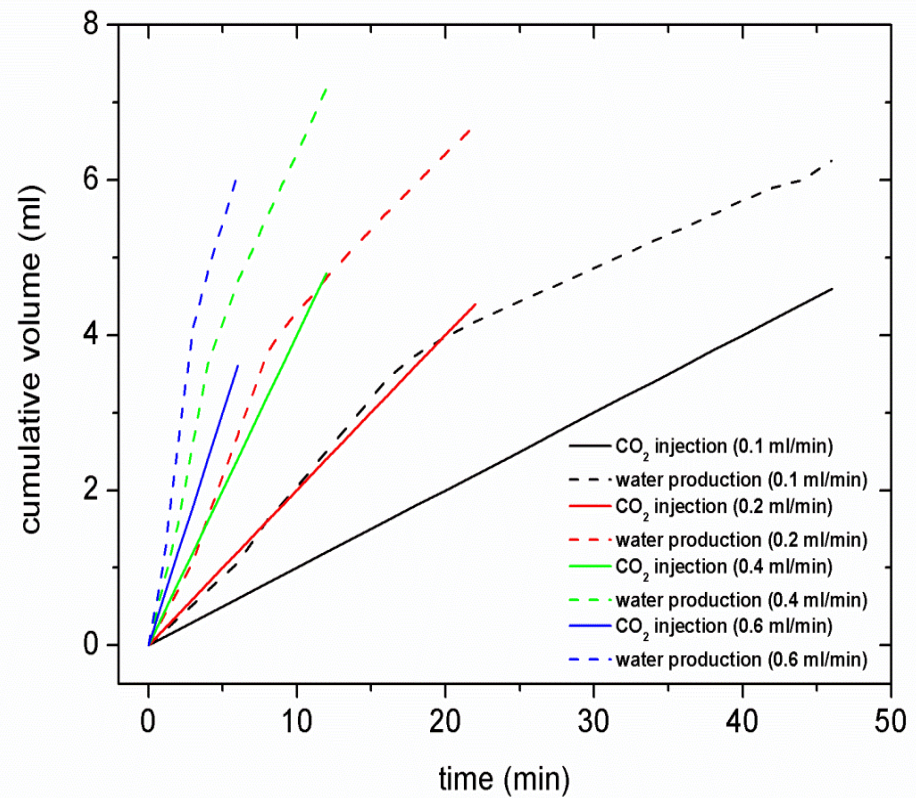
Effect of CO₂ phase on CO₂-water displacement



Effect of CO₂ phase on CO₂-water displacement

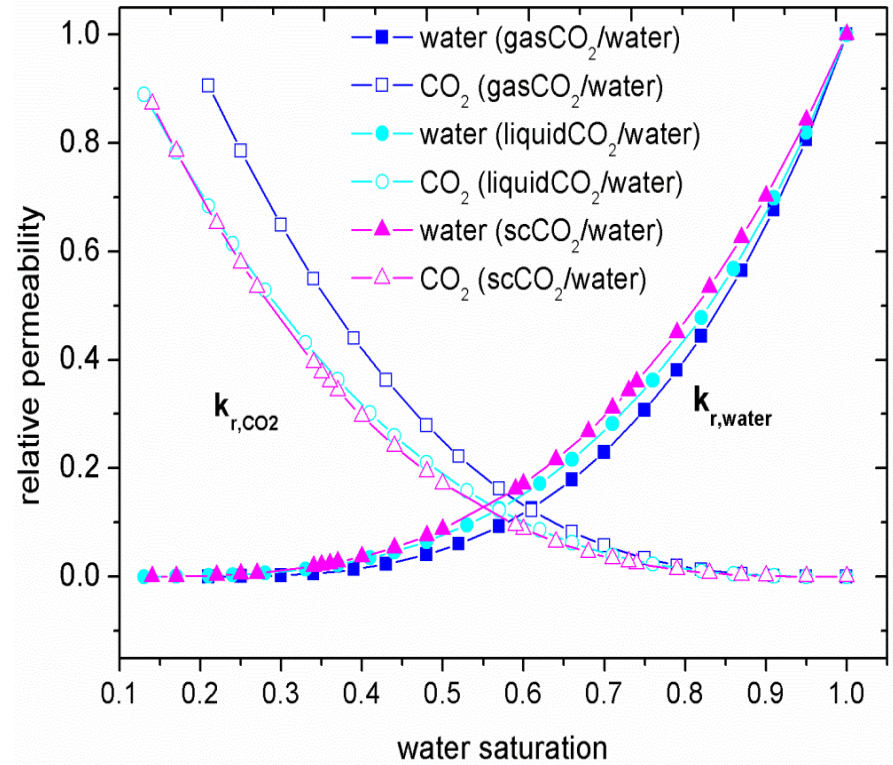
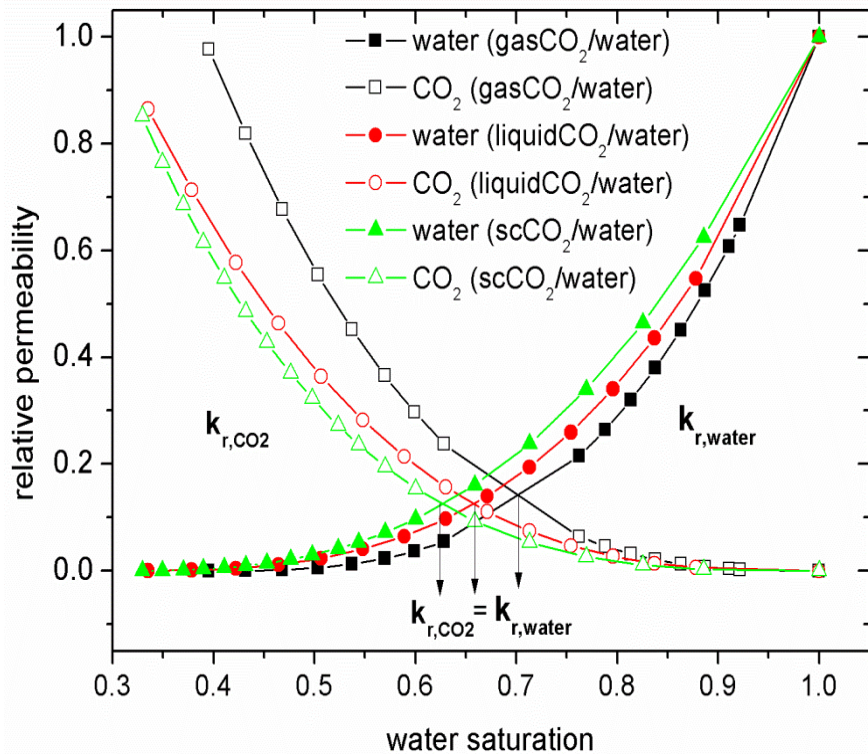


Water production of gas CO₂-water, liquid CO₂-water and supercritical CO₂-water systems



Cumulative water production for the supercritical CO₂-water system at supercritical CO₂ injection rates of 0.1, 0.2, 0.4 and 0.6 ml/min

Effect of CO₂ phase on CO₂-water displacement



Relative permeability curves for gas CO₂-water, liquid CO₂-water and supercritical CO₂-water displacements

Relative permeability curves predicted based on Plug and Bruining's experimental data for gas CO₂-water, liquid CO₂-water and supercritical CO₂-water displacement

Development of a compact process for CO₂ capture

❖ Post-combustion with aqueous technology¹.

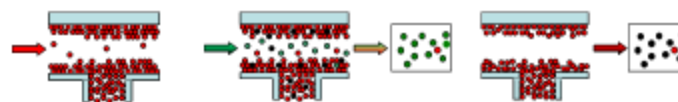
❖ However, the issues arise from the high energy consumption for the desorption

➤ Develop a **compact** CO₂ capture process to deal with increasing

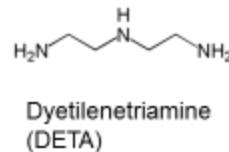
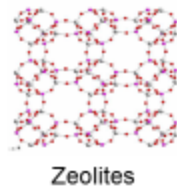
Combination of a rotating packed bed absorber and microwave (MW) assisted thermal regeneration.

Wetting Layer Absorbents

Develop a wetting layer absorption (WLA) carbon capture process based on chemical solvents



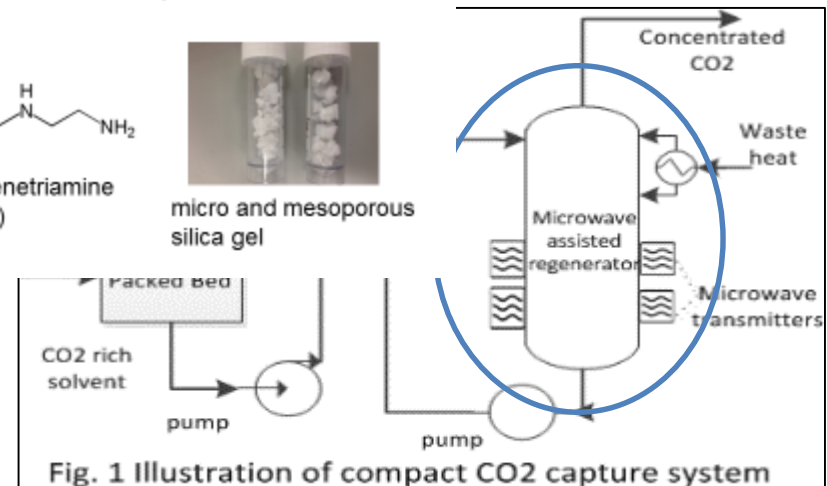
In comparison with liquid amine scrubbing processes, WLA has high working capacity and rate of mass transfer, and lower regeneration penalty



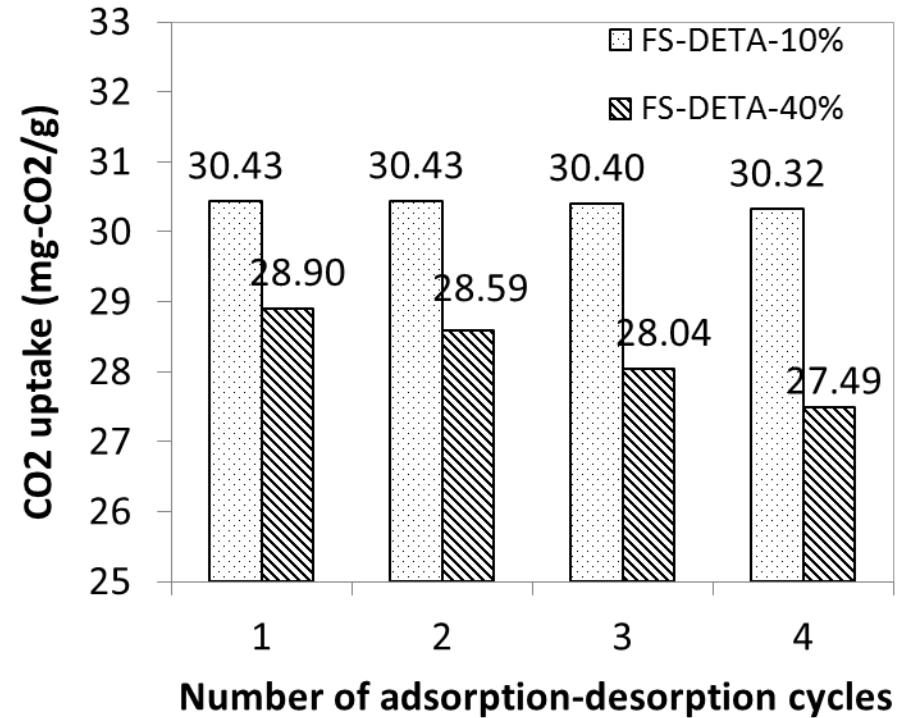
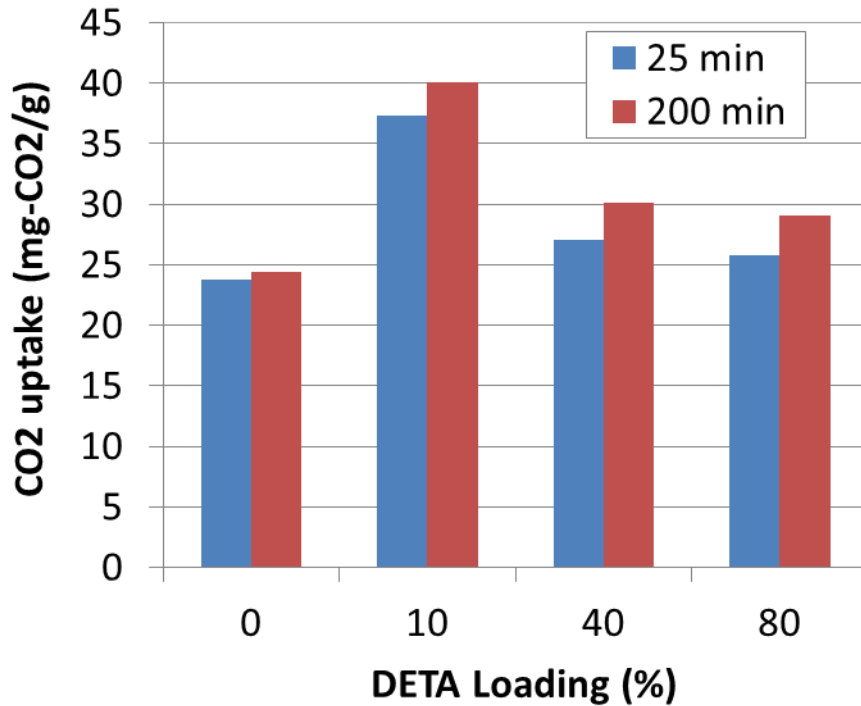
micro and mesoporous silica gel

Commercially available

Low energy consumption for



CO₂ adsorption and regenerability



TGA test results

Development of Fluidization Technique for CO₂ Capture and Combustion

